https://doi.org/10.5194/os-2021-96
Preprint. Discussion started: 7 October 2021

Ocean Science Discussions

Air-sea heat flux during warming season determines the interannual variation of bottom cold water mass in a semi-enclosed bay

Junying Zhu[1], Jie Shi[2,3], Xinyu Guo[4]

[1]College of Marine Sciences, Hainan University, Haikou 570228, China
[2]Key Laboratory of Marine Environment and Ecology, Ocean University of China, Ministry of Education, 238 Songling Road, Qingdao 266100, China
[3]Laboratory for Marine Ecology and Environmental Sciences, Qingdao National Laboratory for Marine Science and Technology, Qingdao 266071, China
[4]Center for Marine Environmental Studies, Ehime University, 2-5 Bunkyo-Cho, Matsuyama 790-8577, Japan

Correspondence to: Xinyu Guo (guoxinyu@sci.ehime-u.ac.jp)

Abstract. A bottom cold water mass (BCWM) is a widespread physical oceanographic phenomenon in coastal seas, and its temperature variability has an important effect on the marine ecological environment. In this study, the interannual variation of the BCWM in Iyo-Nada (INCWM), a semi-enclosed bay in the Seto Inland Sea, Japan, from 1994 to 2015 and its influencing factors were investigated using monthly observational data and a hydrodynamic model. The interannual variation in water temperature inside the INCWM showed a negative correlation with the area of the INCWM, and positive correlations with the local water temperature from April to July and with remote water temperature below 10 m in an adjacent strait in July. Differing from previously studied BCWMs, which had interannual variations depending closely on the water temperature before the warming season, the interannual variation of INCWM depends strongly on the air-sea heat flux during the warming season via local vertical heat transport and lateral heat advection. Further, by comparing several BCWMs, we found that the BCWM size is a key factor in understanding the mechanisms responsible for the interannual variation of BCWMs in coastal seas. These findings will help to predict bottom water temperatures and improve the current understanding of ecosystem changes in shelf seas under global climate change.

1 Introduction

With global climate change, interannual variations in water temperature in coastal oceans are attracting significant attention (Lin et al., 2005; Park et al., 2015; Chen et al., 2020). However, most studies consider sea surface temperature. The lack of long-term observations limits the studies on the bottom water temperature, even though its interannual variations are important for understanding how coastal oceans respond to atmospheric changes (Simpson et al., 2011; Turner et al., 2017).

A bottom cold water mass (BCWM), also called “cold pool”, is the water trapped on the bottom layer as a result of seasonal thermoclines during stratified seasons. It is characterized by lower temperatures than the surrounding waters and has been reported to occur in many shelf seas, such as the Yellow Sea (Wei et al., 2010), Irish Sea (Hill et al., 1994), Middle Atlantic Bight (Lentz, 2017), North Sea (Brown et al., 1999), Bering Sea (Zhang et al., 2012) and Seto Inland Sea (Yu and Guo,

https://doi.org/10.5194/os-2021-96
Preprint. Discussion started: 7 October 2021

2018). As BCWMs occur every year with an annual cycle of forming during the warming season (from spring to summer), being the strongest in summer, and dissipating in early fall, they are good indicators to demonstrate the response of the coastal sea to climate change. In addition, interannual variations in BCWMs have been reported to affect marine ecosystems (Stabeno et al., 2012; Wang et al., 2014; Abe et al., 2015). Therefore, clarifying their interannual variations and controlling factors are helpful for understanding marine ecosystem changes.

Limited by the absence of long-term observations, only the Yellow Sea Cold Water Mass and Middle Atlantic Bight Cold Pool have been studied for their interannual variation and causes (Yang et al., 2014; Coakley et al., 2016; Li et al., 2017; Zhu et al., 2018; Chen and Curchitser, 2020), both of which exhibited apparent interannual variations. Specifically, the interannual variations of the Yellow Sea Cold Water Mass are closely related to the air-sea heat flux in the previous winter (Wei et al., 2010; Park et al., 2011; Li et al., 2015; Zhu et al., 2018). After studying the Middle Atlantic Bight Cold Pool, Chen and Curchitser (2020) suggested that its temperature interannual variations during stratified seasons were controlled by both the previous winter temperature and abnormal warming/cooling due to oceanic advection. Nevertheless, there remains little information regarding the interannual variations of BCWMs in other coastal seas.

The Seto Inland Sea is the largest semi-closed coastal sea in western Japan, with an average depth of 38 m and a surface area of 23,000 km^2 (Fig. 1a). It opens to the Pacific Ocean via Bungo Channel and Kii Channel and is divided into several shallow basins by narrow straits. The presence of a BCWM in summer has been confirmed in several of its wide basins, including the Iyo-Nada (Takeoka et al., 1993; Yu et al., 2016), Suo-Nada (Chang et al., 2009), Hiuchi-Nada (Guo et al., 2004), and Harima-Nada (Chang et al., 2009). This study focuses on the BCWM in Iyo-Nada, which connects the Bungo Channel with the Hayasui Strait, which has a depth of more than 100 m (Fig. 1b). The water temperature in the Hayasui Strait is homogenous throughout the year because of strong tidal mixing (Kobayashi et al., 2006). From May to July, a density-induced gravitational circulation occurs as the bottom water flows from the Hayasui Strait to Iyo-Nada, whereas the surface water flows in the opposite direction. This circulation can be enhanced in July by an abrupt increase in river discharge into the Seto Inland Sea (Yu et al., 2016; Yu and Guo, 2018).

Previous studies have examined the seasonal change in the BCWM in Iyo-Nada (hereafter, we use “INCWM” to denote the Iyo-Nada BCWM). With the development of stratification, the water temperature of the INCWM increases by 8-10 ℃ from early April to August. Yu and Guo (2018) suggested that seasonal warming in the INCWM results from both lateral heat advection from the surrounding water and vertical diffusion from the surface layer, in which lateral heat advection contributes more than vertical diffusion. However, it is still unknown how the INCWM changes under climate change and how these lateral and vertical processes affect the INCWM on an interannual scale.

The remainder of this study is organized as follows. In Section 2, we introduce the long-term observation data and a hydrodynamic model. In Section 3, we describe the interannual variation in the INCWM and its relationship with the surrounding water. In Section 4, we discuss the factors controlling the interannual variation of the INCWM and compare them with those of BCWMs in other coastal seas. Finally, we summarize the main results in Section 5.

https://doi.org/10.5194/os-2021-96
Preprint. Discussion started: 7 October 2021

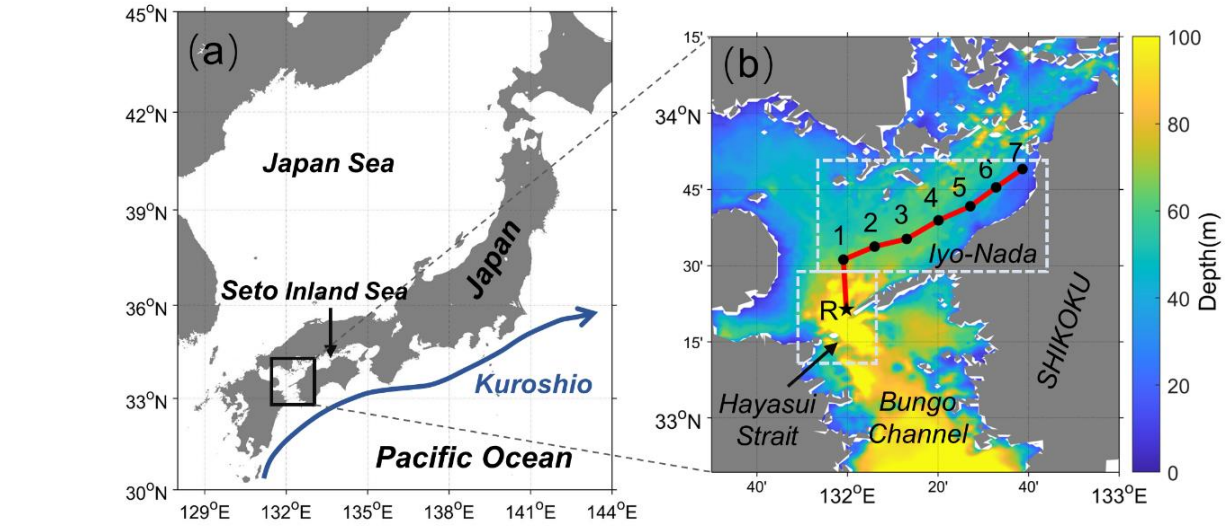

Figure 1: Location of (a) Seto Inland Sea and (b) observation stations. Stations are represented by black dots and stars. The areas enclosed in the dotted boxes in (b) represent Iyo-Nada (131.9-132.8°E, 33.45-33-75°N) and the Hayasui Strait (131.8-132.1°E, 33.15-33-75°N), which were used in the numerical sensitivity experiments.

2 Methods

2.1 Long-term observation data

The Prefectural Fishery Research Centers around the Seto Inland Sea have conducted ship-based hydrographic observations almost every month since 1971 to monitor water quality. For this study, we collected the observed water temperature data from the Iyo-Nada (stations 1-7) and the Hayasui Strait (station R) (Fig. 1b) from 1994 to 2015 (no data for 2000). The data cover depths of 0 m, 10 m, 20 m, and 50 m at all stations as well as additional 75 m deep measurements at station R.

The spatial distributions of multi-year (1994-2015) averaged water temperature along a transection (Station R to Station 7) in January, April, July, and October are shown in Fig. 2a. Overall, the INCWM exhibits a prominent seasonal evolution that forms in April, matures in July, and disappears in October. The seasonal cycle is consistent with that of other BCWMs (Horsburgh et al., 2000; Zhang et al., 2012; Chen et al., 2018; Zhu et al., 2018). The main part of the INCWM in July is located at stations 1-4 and below a depth of 20 m (Fig. 2a). According to the time series of the multi-year (1994-2015) averaged water temperature at the sea surface and 50 m deep for stations 1-4 (Fig. 2b), the water column mixed well from October to March. Meanwhile, the water temperatures at the sea surface and 50 m deep diverged from April to September, during which the water temperature rose at a rate of 3.0 ℃ month^{-1} at the sea surface and 1.8 ℃ month^{-1} at 50 m deep. The water temperature difference between the sea surface and 50 m deep reached 5.5 ℃ in July. Then, enhanced wind and

https://doi.org/10.5194/os-2021-96
Preprint. Discussion started: 7 October 2021

85 surface cooling break this stratification in the fall, and consequently, the INCWM disappears in October. As more typhoons pass through Japan in August than in July (http://www.data.jma.go.jp/obd/stats/data/bosai/tornado/stats/monthly.html), we selected July to examine the interannual variations of the INCWM.

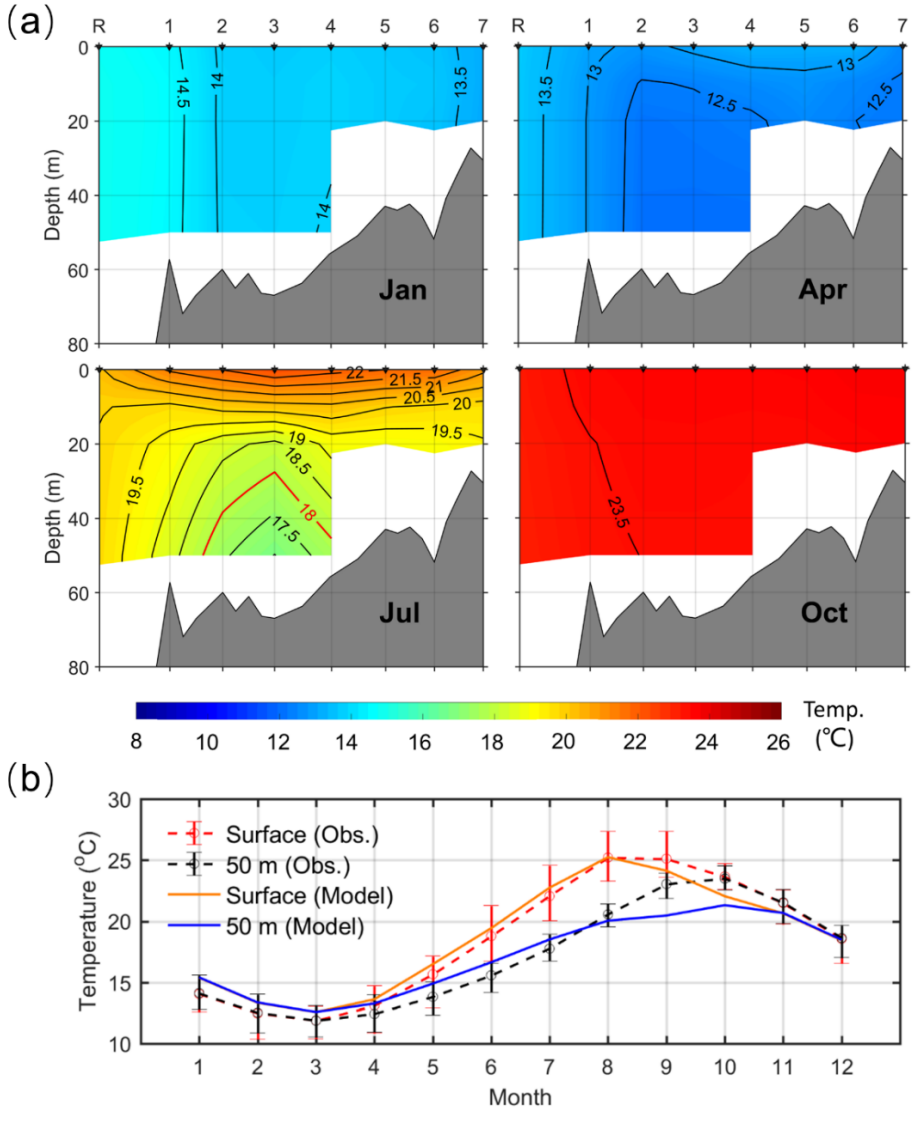

Figure 2: (a) Spatial distributions of multi-year (1994-2015) averaged water temperature along a transect (station R to station 7) in
90 **January, April, July, and October. (b) Time series of observed and simulated water temperatures averaged for stations 1-4 at the surface and 50 m deep. The red line of the 18 °C isotherm in (a) is used to define the Iyo-Nada bottom cold water mass (INCWM). The red and black bars in (b) represent the ranges of observed water temperatures at the surface and 50 m deep, respectively.**

https://doi.org/10.5194/os-2021-96
Preprint. Discussion started: 7 October 2021

The intensity of the INCWM can be defined by the spatially averaged water temperature inside the INCWM and the area of INCWM along the observational transect (Fig. 1b), which was used in Zhu et al. (2018) to study the Yellow Sea bottom cold water. Briefly, X is set to be any of the two indices, and X_0 is the mean value of X from 1994 to 2015. Thus, ΔX_i is the anomaly of X_i at year i:

$$\Delta X_i = X_i - X_0 .$$

The mean range of change over the entire study period is denoted by the mean value of the absolute value of ΔX_i:

$$p = \frac{1}{n}\sum_{i=1}^{n} |\Delta X_i| ,$$

where n is the total number of data points. A strong INCWM year is characterized by a low water temperature and a large area, while a weak INCWM year is characterized by a high water temperature and a small area. When the water temperature anomaly in a year is smaller than its $-0.5p$ and the area anomaly in a year is larger than its $0.5p$, the year is defined as a strong INCWM year. Conversely, when the water temperature anomaly in a year is larger than its $0.5p$ and the area anomaly is smaller than its $-0.5p$, the year is defined as a weak INCWM year. Note that any other situation is defined as a normal INCWM year.

2.2 Model configuration and validation

Herein, we used a three-dimensional hydrodynamic model to examine the factors influencing interannual variation in the INCWM. This model is based on the Princeton Ocean Model, and its configuration is described in detail by Zhu et al. (2019). Note that the sea surface atmospheric forcing used was the multi-year average. Model validations of residual current, water temperature, and salinity in the Seto Inland Sea have been reported in previous studies (Chang et al., 2009; Zhu et al., 2019). As an example of model results related to the INCWM, Fig. 2b shows the seasonal variation of the simulated water temperature at the sea surface and 50 m deep for stations 1-4. It is likely that the model captured the seasonal evolution of the INCWM given by the observed data up to August. However, the difference between the simulated and observed water temperatures increased in September and October. The reason for it is that the model is driven by the multi-year average daily wind field, which cannot fully represent episodic strong wind events, especially typhoons, which are the most active in September and October. Therefore, the kinetic energy input to the ocean is much lower than the realistic situation. However, our simulation target is the formation and maintenance of the BCWM from the previous winter to summer, which is only slightly related to the model results in September and October. Therefore, this model is suitable for examining the factors influencing the interannual variation in the INCWM via sensitivity experiments. The climatological simulation of the INCWM is named CONTROL, and sensitivity experiments are described in Section 4.2.

https://doi.org/10.5194/os-2021-96
Preprint. Discussion started: 7 October 2021


Ocean Science Discussions

2.3 Method quantifying the influence of sea surface forcing on interannual variation of the INCWM

To investigate the response of the INCWM to sea surface forcing changes, we conducted three numerical sensitivity experiments (Table 1). In each sensitivity experiment, the air-sea heat flux over the target area was 10 % different from CONTROL. The sensitivity coefficient q is defined to quantify the response of the INCWM along the transect, as shown in Fig. 1b. Using water temperature as an example, q can be calculated using the following formula:

$$q = \left|\frac{T_{case}-T_{control}}{T_{control}}\right|, \quad (1)$$

where $T_{control}$ is the average water temperature in the area enclosed by a specific isotherm (18 ℃, Fig. 2a, July) in the CONTROL, and T_{case} is the corresponding variable in one of the sensitivity experiments. If there is no water below 18 ℃, the water temperature at the mean location of the INCWM is used for T_{case}.

Table 1: List of numerical experiments and conditions.

Experiments	Conditions
Case1	The surface heat loss in Iyo-Nada in the previous winter increased by 10 %
Case2	The surface heat gain in Iyo-Nada from May to July increased by 10 %
Case3	The surface heat gain in the Hayasui Strait from May to July increased by 10 %

Regarding the interannual variation of INCWM, the influence of sea surface forcing is evaluated not only by the sensitivity coefficient q but also by the changing range of forcing. To quantify the relative contributions of air-sea heat flux to the interannual variation of the INCWM, we first calculate the multi-year mean seasonal variation and then eliminate seasonal change signals in order to obtain the interannual variation sequence in the air-sea heat flux. For a certain period, the standard deviation of the interannual variation sequence ($std(f)$) is used to represent the change range of air-sea heat flux, and its influence cr is evaluated using the results of the sensitivity experiment via the following relationship:

$$\frac{cr}{std(f)} = \frac{q}{\Delta f}, \quad (2)$$

where f is the interannual variation sequence of the air-sea heat flux, which eliminates the seasonal signals, and Δf is the change value in the sensitivity experiment (Table 1) for the air-sea heat flux. For the size of the INCWM, T_{case} and $T_{control}$ in Eq. (1) are replaced by the area enclosed by the 18 ℃ isotherm in the corresponding experiments. If there is no water below 18 ℃, the area of the INCWM is set to 0. The cr can be used to evaluate the relative contribution of the air-sea heat flux to the interannual variation of the INCWM. Meanwhile, $cr(T)$ and $cr(A)$ represent the relative contribution of air-sea heat flux to the temperature and area of the INCWM, respectively.

With the exception of the air-sea heat flux, the contribution of wind stress to the interannual variation of the INCWM was also quantified using the aforementioned method. Note that the forcing values used in this calculation, such as the air-sea heat flux and wind stress during 1994-2012, were derived from the climate dataset DSJRA-55, which is a regional downscaling based on the Japanese 55-year Reanalysis (JRA-55; Kobayashi et al. 2015) (https://jra.kishou.go.jp/), provided

https://doi.org/10.5194/os-2021-96
Preprint. Discussion started: 7 October 2021

by the Japan Meteorological Agency. The data are provided hourly with a horizontal resolution of 5 km to appropriately represent phenomena associated with Japan's uneven terrain (Kayaba et al., 2016).

3 Results

3.1 Interannual variations of the INCWM in July

The temperature is lower inside the INCWM than in its surrounding waters. The lowest observed temperature in July along the transect in Iyo-Nada (Fig. 1b) was 15.74-18.23 ℃ during 1994-2015. The boundary of INCWM was defined by the 18 ℃ isotherm in July (Fig. 2a), and the average water temperature and area inside the 18 ℃ isotherm were calculated. As shown in Fig. 3, there was a prominent interannual variation in the water temperature and area of the INCWM. The lowest average water temperature in the INCWM was 17.04 ℃ in 2006. Meanwhile, the multi-year average temperature of the INCWM was 17.58 ℃ with a standard deviation of 0.27 ℃. Overall, consistent interannual variation was observed for the average and lowest water temperature of the INCWM (figure not shown), exhibiting a correlation coefficient of 0.98 ($p < 0.01$).

A significant negative correlation ($r = -0.86$, $p < 0.01$) was found between the average water temperature and the area of the INCWM, indicating that when the water temperature of the INCWM is low in a year, the area of the INCWM is large and the INCWM intensity is strong. As a result, the INCWM was strong in 1994, 1996, 2006, 2010, 2012, 2013, and 2015, and weak in 1997, 2003, 2004, 2007, 2009, 2011, and 2014 (Fig. 3).

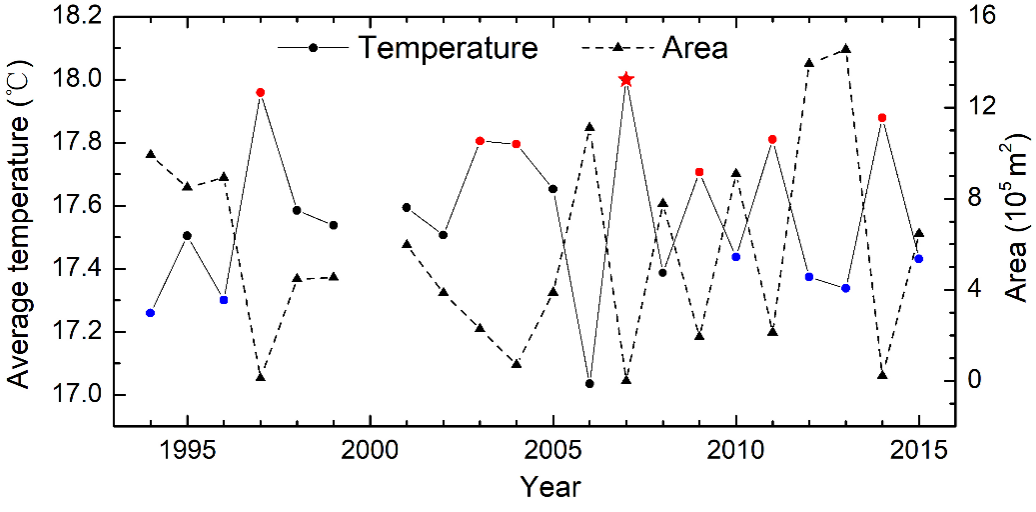

Figure 3: Time series of mean water temperature (solid line) and area (broken line) of the Iyo-Nada bottom cold water mass (INCWM) in July during 1994-2015. A strong INCWM year is marked by blue circles, while a weak INCWM year is marked by red circles. The red star indicates that we did not identify a BCWM in 2007 because the water temperature was higher than 18 ℃ along the entire transect. For this case, we used the observed temperature (18.23 ℃) at the average location of the INCWM (50 m deep at station 3) as the average temperature and specified a zero area.

https://doi.org/10.5194/os-2021-96
Preprint. Discussion started: 7 October 2021

3.2 Correlation between INCWM with surrounding waters

As shown in Fig. 2b, the water temperature at the place of the INCWM was homogeneous in January before gradually forming a distinct dome under the sea surface heating during spring and summer. To explore the influence of the water temperature at different stages during its formation process on the intensity of INCWM in July, we calculated the correlation coefficients between the average temperature of the INCWM in July (Fig. 3) and the water temperatures at all the depths of each station from 1994 to 2015 for each month (from previous December to July).

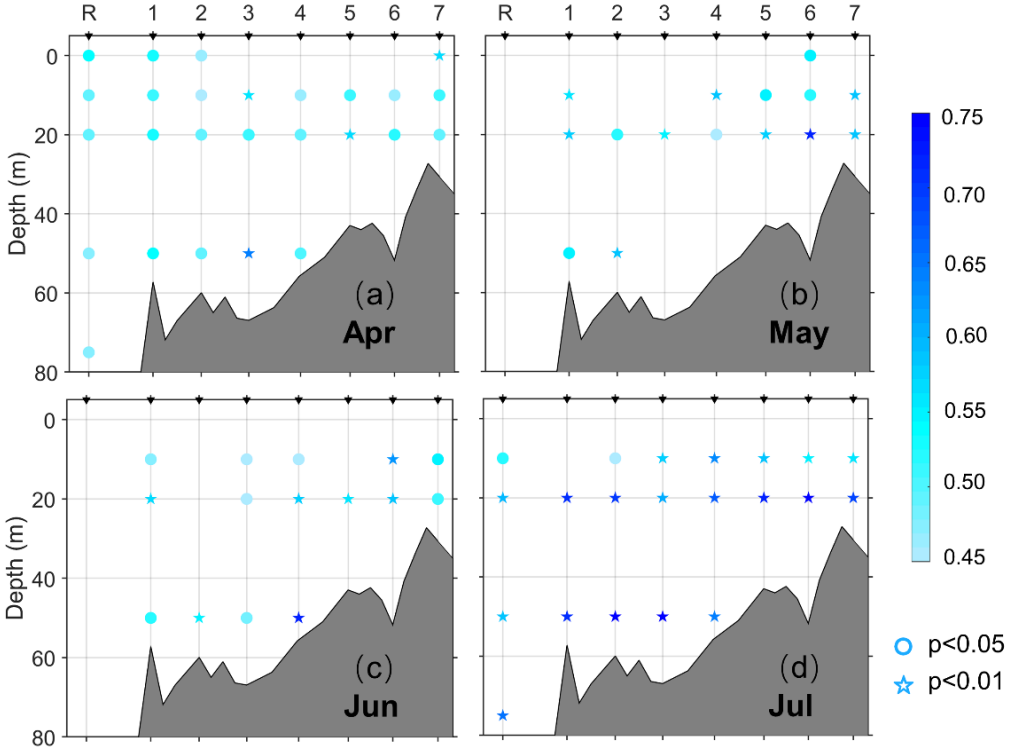

Figure 4: Correlation coefficients for interannual variation of water temperature at each station from April to July and that of the Iyo-Nada bottom cold water mass (INCWM) mean water temperature in July during 1994-2015. Circles indicate that the significant difference level is more than 0.95, and stars indicate a significant difference level of more than 0.99.

Overall, more significant correlations appeared from April to July (Fig. 4) than from previous December to March. In April, the water temperatures at almost all stations and depths were significantly correlated with the average water temperature of the INCWM in July (Fig. 4a). From May to July (Figs. 4b-d), although the significant correlations at the sea surface and

https://doi.org/10.5194/os-2021-96
Preprint. Discussion started: 7 October 2021

station R disappeared, the water temperature below 10 m at stations 1-7 still showed significant correlations with the average water temperature of the INCWM in July. The relationship among all the stations and depths was likely enhanced in July, as shown by the correlation coefficients larger than 0.60 ($p < 0.01$) (Fig. 4d). In addition, a significant correlation below 10 m at station R was observed in July but disappeared in May and June, indicating a distinct connection in July between the interannual variation of the INCWM and the water around station R, which is the Hayasui Strait.

3.3 Processes influencing the interannual variations of the INCWM

According to the seasonal evolution of the INCWM, the difference in water temperature between the sea surface and 50 m deep begins in April (Fig. 2b). The water temperature in April was selected as the initial value for the formation of the INCWM in the following months. The significant correlations shown in Fig. 4 demonstrate that the local water temperature below 10 m in April is closely related to the interannual variation of the INCWM in July. Because the water temperature in April depended mainly on the cooling process, the initial temperature of the INCWM is likely associated with local air-sea heat flux from winter to early spring.

During the warming season, the effect of local water temperatures below 10 m persists. The correlation coefficient below 10 m is larger in May-July than in April (Figs. 4b-d), indicating that heat transport into the INCWM from May to July is also important for the interannual variation of the INCWM in July. Using the temperature difference between the sea surface and 20 m depth at stations 1-4 as the thermocline strength, a significant negative correlation ($r = -0.44$, $p < 0.05$) was obtained for the thermocline strength in July and the average water temperature of the INCWM in July, indicating that a stronger thermocline strength corresponds to a stronger INCWM. Because there is no significant correlation between the INCWM and sea surface temperature at stations 1-5 from May to July (Fig. 4), the stronger thermocline strength acts to reduce the downward heat transport from the sea surface to the INCWM.

In addition, river discharge around the Seto Inland Sea increases during the warming season, facilitating the occurrence of an estuarine-like density circulation with the bottom flow from the Hayasui Strait to Iyo-Nada, which ultimately promotes horizontal heat transport into the INCWM (Yu and Guo, 2018). When river discharge reaches a peak in July (Zhu et al., 2019), the bottom horizontal density flow is enhanced, causing more heat to be laterally transported to the INCWM in July than in other months. This process is supported by the significant correlation coefficient of approximately 0.6 ($p < 0.01$) (Fig. 4d) below 10 m at station R in July. Therefore, the lateral heat transport from the Hayasui Strait to Iyo-Nada is another important process that influences the interannual variation of the INCWM in July.

Based on these findings, the interannual variation in INCWM temperature is not only dependent on the initial water temperature before its formation but also on the heat transport processes (horizontal and vertical) during warming seasons. As shown in Fig. 5, a strong INCWM (surrounded by gray dotted line) corresponds to a combination of a low local initial water temperature in April (11.0-12.5 ℃) and a low water temperature at 10-50 m deep at station R in July (19.5-20.3 ℃). Conversely, a weak INCWM usually corresponds to a combination of a high local initial water temperature in April (11.7-14.1 ℃) and a high water temperature (19.8-20.9 ℃) in the Hayasui Strait at depths of 10-50 m in July. Since the local

https://doi.org/10.5194/os-2021-96
Preprint. Discussion started: 7 October 2021

vertical heat transport is not included in Fig. 5, it is not easy to address the relative importance of each process to the interannual variation of the INCWM from only observations.

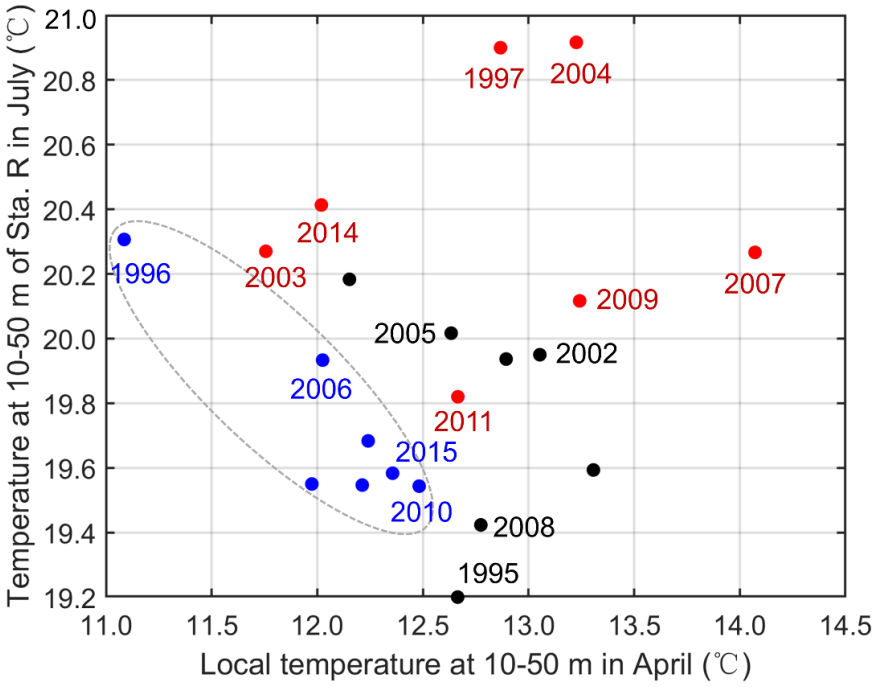

Figure 5: Scatter plot for the Iyo-Nada bottom cold water mass (INCWM) strength (color) according to local water temperature below 10 m in April (x-axis) and water temperature below 10 m at station R in July (y-axis). Blue, black, and red solid circles represent strong, normal, and weak INCWM years, respectively, which is consistent with the results found in Fig. 3.

4 Discussion

4.1 Contribution of sea surface forcing to interannual variation of the INCWM

Global climate change affects coastal seas via regional sea surface forcing. Air-sea heat flux is the main heat source to the Seto Inland Sea (Tsutsumi and Guo, 2016) and affects each stage of the INCWM by directly local input or remote input through horizontal heat transport from adjacent areas. Based on the climatological simulation of the INCWM described in Section 2.2 (CONTROL), we conducted three numerical experiments (Table 1) to address the relative contribution of local and remote air-sea heat flux to the interannual variation of the INCWM in July. The Seto Inland Sea loses heat in winter and gains heat in summer. To determine the effects of local heat flux at different stages of the INCWM, we increased the air-sea heat flux loss/gain over Iyo-Nada (light blue dotted box in Fig. 1b) by 10 % from previous December to February (cooling season) in Case 1 and from May to July (warming season) in Case 2. In addition, to determine the effects of remote heat flux,

https://doi.org/10.5194/os-2021-96
Preprint. Discussion started: 7 October 2021

we increased the air-sea heat flux over the Hayasui Strait (light blue dotted box in Fig. 1b) by 10 % from May to July in Case 3.

As listed in Table 2, both the sensitivity coefficients q of water temperature and area of the INCWM were much higher in Case 2 and Case 3 than in Case 1, indicating that the air-sea heat flux was more important in the warming season than in the cooling season. Regarding the interannual variation range of air-sea heat flux, the relative contributions of water temperature ($cr(T)$) and area ($cr(A)$) to the INCWM revealed some disagreement. For water temperature, the contributions of local and remote air-sea heat flux during the warming season were approximately 4.0 and 2.5 times, respectively, those during the cooling season, suggesting that the heat transport in the warming season is the dominant process influencing the interannual variation of the INCWM water temperature in July, to which the local air-sea heat fluxes contribute a little more than the remote air-sea heat fluxes. With respect to area, the $cr(A)$ in Case 1 was slightly larger than those in Case 2 and Case 3, indicating the importance of the winter cooling process. From three numerical experiments, we conclude that the vertical and horizontal heat transport processes in the warming season, rather than the initial condition preserved from the previous winter, are responsible for interannual variation in the INCWM in July.

Table 2: Contributions of air-sea heat flux to interannual variation of the bottom cold water mass in Iyo-Nada (INCWM) in numerical experiments.

Experiments	Sensitivity coefficient q		Variation of the air-sea heat flux ($std(f)$)	Variation in experiments (Δf)	cr	
	Temp.	Area			$cr(T)$	$cr(A)$
Case 1	1.99×10^{-3}	0.35	65.35	13.69	9.49×10^{-3}	1.67
Case 2	2.47×10^{-2}	1.00	22.17	14.26	3.84×10^{-2}	1.55
Case 3	1.57×10^{-2}	0.87	22.77	14.58	2.44×10^{-2}	1.28

Note: As the area of INCWM is 0 in Case 2, the sensitivity coefficient of the area is 1.00.

Wind-induced surface mixing is another factor affecting vertical heat transport. Thus, we conducted the same numerical experiments we did for air-sea heat flux for wind stress. However, the sensitivity coefficients q of wind were less than 0.006 and 0.06 for the temperature and area of the INCWM, respectively, which were much smaller than those of the air-sea heat flux experiments (Table 2). The weak sensitivity to wind stress is because of the presence of essential weak wind during the warming season in the study area. Consequently, air-sea heat flux is the main atmospheric forcing influencing interannual variation in the INCWM in July.

4.2 Comparison with BCWMs in other coastal seas

We investigated the interannual variation of a BCWM in a semi-enclosed coastal sea in Japan using long-term observations and a hydrodynamic model. As previously mentioned, BCWMs have been reported in continental seas worldwide. Overall,

https://doi.org/10.5194/os-2021-96
Preprint. Discussion started: 7 October 2021

most of their seasonal evolutions and formation mechanisms, for example, being a part of remnant water from the previous winter, are similar (Horsburgh et al., 2000; Zhang et al., 2012; Lentz, 2017; Yu and Guo, 2018). Thus, we compared several coastal sea BCWMs regarding their interannual variation.

The interannual variations of the Middle Atlantic Bight Cold Pool and Yellow Sea Cold Water Mass and their influencing factors have been described by Chen and Curchitser (2020) and Zhu et al. (2018). Compared with these BCWMs, the coherent negative relationship between water temperature and size of BCWM was preserved in our study area, indicating a strong BCWM year featuring a low water temperature and a large size (area or volume). Therefore, as an essential feature of a BCWM, its water temperature and size (area and volume) experience a consistent relationship among different coastal seas, presenting an inherent property that the water temperature inside the BCWM has a negative correlation with the spatial scale of the BCWM over an interannual time scale. Specifically, when heat enters the BCWM from the surrounding water, the water temperature inside the BCWM increases, causing the boundary of the BCWM defined by a specific water temperature to shrink.

Although similarly distinct interannual variations have been observed for these three BCWMs (Yellow Sea Cold Water Mass, Middle Atlantic Bight Cold Pool, and INCWM), their major causes are different. Zhu et al. (2018) suggested that interannual variation in the Yellow Sea Cold Water Mass in summer depends mainly on the water temperature in the previous winter, which is controlled by local air-sea heat flux during the cooling season. Chen and Curchitser (2020) suggested that the temperature anomaly during winter and spring (mid-January to March) is the primary factor responsible for the interannual variability of the Middle Atlantic Bight Cold Pool temperature during the stratified season. Therefore, for these BCWMs, the initial temperature associated with the air-sea heat flux during the cooling season is important to their interannual variation in summer. However, in this study, we found that the vertical and horizontal heating processes during the warming season, rather than the initial temperature before warming, were the dominant factor for interannual variation in the INCWM. This indicates that the primary influencing process on BCWMs interannual variation can vary, even though their seasonal cycles and formation processes are similar.

Interannual variation in BCWM temperature consists of two parts: the initial temperature after the cooling season, and the increasing range during the warming season. Because the water column vertically mixes in winter, the initial temperature of the BCWM is closely related to the local air-sea heat flux during the cooling season (Chen et al., 2016; Zhu et al., 2018). The increasing range of water temperature inside the BCWM during the warming season is controlled by the heat input from the surrounding water.

As an approximation, we assume that a BCWM has the simple form of a cylinder with radius R (i.e., horizontal range of BCWM) and height H (i.e., average thickness of BCWM). The initial water temperature of the BCWM is homogenous and the vertical heat diffusion coefficient is a constant. Further, during the warming season, the heat exchange flux with the surrounding water caused by sea surface heat flux is a constant m, and that caused by lateral heat flux is a constant n. Thus, on a seasonal scale, the following two equations can be established according to the conservation principle of heat:

https://doi.org/10.5194/os-2021-96
Preprint. Discussion started: 7 October 2021

$$\rho V C_p \frac{dT_1}{dt} = m \cdot \pi R^2 , \quad (3)$$

$$\rho V C_p \frac{dT_2}{dt} = n \cdot 2\pi R \cdot H , \quad (4)$$

where T_1 is the BCWM temperature change caused by sea surface heat flux, T_2 is the BCWM temperature change caused by lateral heat flux. ρ is the seawater density, C_p is the heat capacity, and V is the volume of the cylinder ($V = \pi R^2 H$). Using Eq. (3) and Eq. (4), we can obtain the following relationship:

$$\frac{dT_1}{dt} \propto \frac{m}{H} , \frac{dT_2}{dt} \propto \frac{2n}{R} , \quad (5)$$

Equation (5) reveals that temperature change in the BCWM caused by sea surface heat flux is inversely proportional to H and that caused by lateral heat flux is inversely proportional to R. If we use T to represent the temperature of the BCWM, then its variation during the warming season can be given as:

$$\frac{dT}{dt} = \frac{dT_1}{dt} + \frac{dT_2}{dt} = \frac{1}{\rho C_p}\left(\frac{m}{H} + \frac{2n}{R}\right) , \quad (6)$$

$\frac{dT}{dt}$ is inversely proportional to the size of BCWM (H and R), suggesting that the larger the size of the BCWM, the smaller the BCWM temperature changes during the warming season.

On this basis, we collected the information of five BCWMs (Table 3). The horizontal size of the BCWMs (R) varies widely from 40 km×30 km (Iyo-Nada) to 500 km×300 km (Bering Sea), whereas the average thickness of BCWMs (H) changes from around 30 m to 50 m. Because the horizontal size of the BCWMs and their variation are much larger than those in the vertical size, the water temperature variation of BCWM depends mainly on R.

As listed in Table 3, the water temperature rising rate during the warming season increases with decreasing horizontal BCWM size, which is consistent with the previous analysis. Therefore, the importance of local initial water temperature after a cooling season on the BCWM's temperature in summer is enhanced with an increase in the horizontal size of the BCWM. Note that the rate of temperature increase in the Middle Atlantic Bight Cold Pool is the same as that of the BCWM in the Irish Sea, although the size of the Middle Atlantic Bight Cold Pool is larger (Table 3). Such difference is the result of an along-isobath mean current of 5 cm s^{-1} in the Middle Atlantic Bight that develops with the cold pool (Lentz, 2017), which leads to increased heat advection into the cold pool. For Iyo-Nada, the INCWM is adjacent to a strait and the relatively strong horizontal density current exists between the strait and BCWM, thereby increasing the rate of temperature rise in the INCWM during the warming season (Yu et al., 2016).

https://doi.org/10.5194/os-2021-96
Preprint. Discussion started: 7 October 2021

320 **Table 3 Characteristics of bottom cold water mass (BCWMs) in five coastal seas.**

Coastal seas	Horizontal size of BCWM (km^2)	Average thickness of BCWM (m)	Temperature rising rate during warming season (°C $month^{-1}$)	Main factor influencing interannual variation in the BCWM	References
Bering Sea	500 km×300 km	50	< 0.15	--	Goes et al. (2014); Wang and Zhao (2011)
Yellow Sea	300 km×300 km	40	approximately 0.2	Air-sea heat flux in the previous winter	Zhu et al. (2018)
Middle Atlantic Bight	100 km×300 km	50	approximately 1.2	Initial winter temperature and abnormal warming/cooling due to advection during stratified seasons	Lentz (2017); Chen et al. (2018)
Irish Sea	100 km×100 km	50	approximately 1.2	--	Holt and Proctor (2003)
Iyo-Nada	40 km×30 km	30	approximately 1.8	Air-sea heat flux during stratified seasons	Yu and Guo (2018); this study

https://doi.org/10.5194/os-2021-96
Preprint. Discussion started: 7 October 2021

Considering the influencing factors on the interannual variation of the three BCWMs (Yellow Sea Cold Water Mass, Middle Atlantic Bight Cold Pool, and INCWM), BCWM size may also be a key factor. As listed in Table 3, for a large size BCWM (such as Yellow Sea Cold Water Mass), the initial temperature is the dominant factor of interannual variation (Zhu et al., 2018) because of the low rate of temperature increase during the warming season. For a small BCWM (such as INCWM), atmospheric forcing (such as air-sea heat flux) during the warming season has a greater effect on interannual variation because of the large heat exchange rate with surrounding waters that are sensitive to atmospheric forcing. For the Middle Atlantic Bight Cold Pool, which is between the Yellow Sea Cold Water Mass and INCWM, both initial temperature and abnormal warming/cooling due to advection during the warming season are its primary drivers (Chen and Curchitser, 2020). Here, we considered the influence of air-sea heat flux and lateral heat flux on the interannual variation of the BCWM temperature according to Eq. (6). For a BCWM of a certain size (H and R are constant), the interannual variation of $\frac{dT}{dt}$ during the warming season ($\Delta\frac{dT}{dt}$) is calculated as follows:

$$\Delta\frac{dT}{dt} = \frac{1}{\rho C_p}\left(\frac{\Delta m}{H} + \frac{2\Delta n}{R}\right) = \frac{1}{\rho C_p}\cdot\frac{\Delta m\cdot R + 2\Delta n\cdot H}{HR}, \quad (7)$$

where Δm is the variation value of air-sea heat flux on an interannual scale, and Δn is the variation in the lateral heat flux on an interannual scale. Note that the influence of Δm is increased by R, while the influence of Δn is increased by H. As R is much larger than H (at least 1000 times), the influence of Δm is supposed to be more important than that of Δn. Furthermore, the importance of air-sea heat flux during the warming season on the interannual variations of the five BCWMs was discussed.

According to Eq. (5), the temperature change in a BCWM caused by the interannual variation of air-sea heat flux is proportional to $\frac{\Delta m}{H}$ (W m^{-3}), which can be used to compare the contribution of air-sea heat flux during the warming season to the interannual variation of BCWMs in different coastal seas. Monthly air-sea heat flux (total of surface net solar radiation, surface net thermal radiation, surface latent heat flux, and surface sensible heat flux) data during 1979-2020 from the ERA5 dataset (https://www.ecmwf.int/en/forecasts/datasets/reanalysis-datasets/era5, spatial resolution of 0.25°×0.25°) were used in the calculation. We used the standard deviation of air-sea heat flux during the warming season (from May to July) to address Δm (Fig. 6). Overall, Δm in the five coastal seas ranged from 7.0 W m^{-2} (Yellow Sea) to 11.4 W m^{-2} (Middle Atlantic Bight) (Fig. 6a). After the adjustment of BCWMs thickness (H), the value of $\frac{\Delta m}{H}$ (approximately 0.27 W m^{-3}) was the biggest in Iyo-Nada, followed by the Middle Atlantic Bight (approximately 0.23 W m^{-3}), and the smallest value (approximately 0.17 W m^{-3}) occurred in the Yellow Sea (Fig. 6b). It has been suggested that the air-sea heat flux during the warming season is more important for the interannual variation of the INCWM than that of the Middle Atlantic Bight Cold Pool and the Yellow Sea Cold Water Mass. Thus, a distinct effect of the BCWM thickness was addressed, especially for the INCWM, which has a thin H (approximately 30 m) (Table 3) and small Δm (Fig. 6a). Regarding the interannual variation of the Yellow Sea Cold Water Mass, the contribution of air-sea heat flux during the warming season was the smallest among the five BCWMs,

https://doi.org/10.5194/os-2021-96
Preprint. Discussion started: 7 October 2021

suggesting the importance of local initial water temperature, which is supported by the results of previous studies (Wei et al., 2010; Li et al., 2015; Zhu et al., 2018). For the BCWMs in the Bering Sea and the Irish Sea, it was inferred that the contribution of air-sea heat flux during the warming season is between that of the Yellow Sea and the Middle Atlantic Bight (Fig. 6).

About the relative importance of vertical heat diffusion and horizontal heat advection during the warming season, it depends closely on local features, including the topography of each coastal sea, and therefore must be clarified case by case. For the INCWM, the results show that the local air-sea heat flux that affects vertical diffusion of heat is more important than the remote air-sea heat flux that affects horizontal heat advection (Table 2).

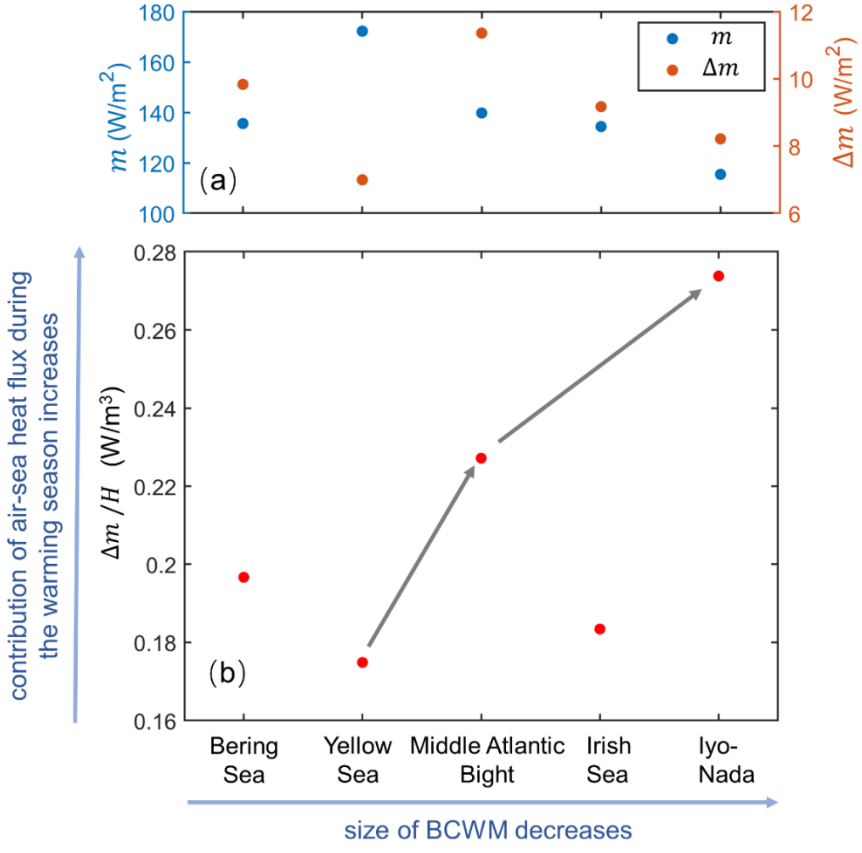

Figure 6: Values of (a) air-sea heat flux during warming season (m) and corresponding interannual variation (Δm), and (b) $\frac{\Delta m}{H}$ values in the five coastal seas. The directions of gray arrows in (b) indicate an increased contribution of air-sea heat flux during the warming season to interannual variation in the bottom cold water mass (BCWM).

https://doi.org/10.5194/os-2021-96
Preprint. Discussion started: 7 October 2021

5 Conclusions

In this study, we investigated the interannual variation of the INCWM from 1994 to 2015 using observational data along a transect across the INCWM. We further analyzed the influencing factors and quantified the contribution of sea surface forcing to interannual variation in the INCWM. The interannual variation of the mean water temperature inside the INCWM and that of its area show a significant negative correlation. The interannual variation of water temperature inside the INCWM depends on both the water temperature in April and the heat transport into the INCWM during the warming season. A strong INCWM corresponds to a low local water temperature in April and a low water temperature in the Hayasui Strait in July. Numerical experiments showed that the air-sea heat flux during the warming season plays a key role in the interannual variation of the INCWM, contributing 6.6 and 1.7 times to the mean water temperature and area of INCWM, respectively, than the air-sea heat flux in the cooling season. Therefore, with respect to interannual variation in the INCWM, the heat transport process during the warming season is more important than the initial temperature after the cooling season. Conversely, for the Yellow Sea Cold Water Mass, the initial temperature after the cooling season is more important than heat transport during the warming season. This difference is likely related to the size of the BCWMs. A larger BCWM has a weaker dependence on heat transport during the warming season, but a stronger dependence on the initial water temperature before the warming season. This simple relationship will be helpful for understanding the responses of bottom water in different coastal seas to changes in atmospheric forcing.

BCWM is a widespread physical oceanic phenomenon. This study examined the interannual variation of water temperature and its controlling factor for a BCWM in the Seto Inland Sea. As an extension, we analyzed the control processes on interannual variation of water temperature in the five BCWMs reported in the literatures using a cylinder column to represent their shape. Our analysis results are consistent with previous studies on the interannual variations of the Yellow Sea Cold Water Mass and the Middle Atlantic Bight Cold Pool. For other BCWMs, although there is no study on their interannual variations, this study provides a direction to know the influencing factor on the interannual variation of water temperature. On the other hand, our simplification with a cylinder column to represent the BCWMs does not consider the variation in bathymetry, which is however expected to affect the current structure around the BCWMs. Although this issue is difficult, it should be one of our future research topics. Another issue is the biogeochemical aspects around the BCWMs, especially the transport of nutrient across the BCWMs, which has considerable effects on the phytoplankton growth around the BCWMs. This is an inverse pathway to the heat transport and is expected to be large in some BCWMs.

Code availability. The source code of numerical model used in this study is available on request. Please contact Xinyu Guo (guoxinyu@sci.ehime-u.ac.jp)

Data availability. The sea surface forcing used for calculation in Section 4 are from DSJRA-55 product (https://jra.kishou.go.jp/) provided by Japan Meteorological Agency and ERA5 product (https://www.ecmwf.int/en/forecasts/datasets/) provided by ECMWF. The observation data is collected from the Prefectural

Fishery Research Centers around the Seto Inland Sea which is available on request. Please contact Xinyu Guo (guoxinyu@sci.ehime-u.ac.jp)

Author contribution. Junying Zhu: Conceptualization, Investigation, Methodology, Data curation, Formal analysis, Software, Validation, Visualization, Writing – original draft preparation, Writing – review & editing; Jie Shi: Conceptualization, Investigation, Methodology, Data curation, Formal analysis, Writing – original draft preparation, Writing – review & editing; Xinyu Guo: Conceptualization, Methodology, Resources, Software, Validation, Supervision, Writing – review & editing

Competing interests. The authors declare that they have no conflict of interest.

Acknowledgements. This study was supported by the Key Research and Development Program of Hainan Province (ZDYF2020203) and the initial fund from Hainan University for Research and Development (KYQD(ZR)21002). Guo X. was supported by the Environment Research and Technology Development Fund JPMEERF20205005 of the Environmental Restoration and Conservation Agency of Japan. Zhu J. was partly supported by the Ministry of Education, Culture, Sports, Science and Technology, Japan (MEXT) under a Joint Usage/Research Center, Leading Academia in Marine and Environment Pollution Research (LaMer) Project. We would like to thank Editage (www.editage.cn) for English language editing.

References

Abe, K., Tsujino, M., Nakagawa, N., and Abo, K.: Characteristic of Si: P: N ratio in bottom water in central Suo-Nada, western Seto Inland Sea, J. Oceanogr., 71, 53-63, https://doi.org/10.1007/s10872-014-0262-4, 2015.

Brown, J., Hill, A. E., Fernand. L., and Horsburgh, K. J.: Observations of a seasonal jet-like circulation at the central North Sea cold pool margin, Estuar. Coast. Shelf S., 48(3), 343-355, https://doi.org/10.1006/ecss.1999.0426, 1999.

Chang, P. H., Guo, X., and Takeoka, H.: A numerical study of the seasonal circulation in the Seto Inland Sea, Japan, J. Oceanogr., 65, 721-736, https://doi.org/10.1007/s10872-009-0062-4, 2009.

Chen, K., Kwon, Y. O., and Gawarkiewicz, G.: Interannual variability of winter-spring temperature in the Middle Atlantic Bight: Relative contributions of atmospheric and oceanic processes, J. Geophys. Res. Oceans, 121, 4209–4227, https://doi:10.1002/2016JC011646, 2016.

Chen, Z., and Curchitser, E. N.: Interannual variability of the Mid-Atlantic Bight Cold Pool, J. Geophys. Res. Oceans, 125, e2020JC016445, https://doi.org/10.1029/2020JC016445, 2020.

Chen, Z., Curchitser, E., Chant, R., and Kang, D.: Seasonal variability of the cold pool over the Mid-Atlantic Bight continental shelf, J. Geophys. Res. Oceans, 123, 8203-8226, https://doi.org/10.1029/2018JC014148, 2018.

Chen, Z., Kwon, Y.O., Chen, K., Fratantoni, P., Gawarkiewicz, G., and Joyce, T. M.: Long-term SST variability on the northwest Atlantic continental shelf and slope, Geophys. Res. Lett., 47, e2019GL085455., https://doi.org/10.1029/2019GL085455, 2020.

https://doi.org/10.5194/os-2021-96
Preprint. Discussion started: 7 October 2021

Coakley, S. J., Miles, T., Kohut, J., and Roarty, H.: Interannual variability and trends in the Middle Atlantic Bight cold pool, Oceans MTS/IEEE, Monterey2016 IEEE 1-6, https://doi.org/10.1109/OCEANS.2016.7761184, 2016.

Goes, J. I., Gomes, H., Haugen, E. M., McKee, K.T., D'Sa, E.J., Chekalyuk, A. M., Stoecker, D. K., Stabeno, P. J., Saitoh, S., and Sambrotto, R. N.: Fluorescence, pigment and microscopic characterization of Bering Sea phytoplankton community structure and photosynthetic competency in the presence of a Cold Pool during summer, Deep Sea Res. II, 109, 84-99, https://doi.org/10.1016/j.dsr2.2013.12.004, 2014.

Guo, X., Futamura, A., and Takeoka, H.: Residual currents in a semi-enclosed bay of the Seto Inland Sea, Japan, J. Geophys. Res. Oceans, 109, https://doi.org/10.1029/2003JC002203, 2004.

Hill, A. E., Durazo, R., and Smeed, D. A.: Observations of a cyclonic gyre in the western Irish Sea, Cont. Shelf Res., 14, 479-490, https://doi.org/10.1016/0278-4343(94)90099-X, 1994.

Holt, J., and Proctor, R.: The role of advection in determining the temperature structure of the Irish Sea, J. Phys. Oceanogr., 33, 2288-2306, https://doi.org/10.1175/1520-0485(2003)033<2288:TROAID>2.0.CO;2, 2003.

Horsburgh, K. J., Hill, A. E., Brown, J., Fernand, L., Garvine, R. W., and Angelico, M. M. P.: Seasonal evolution of the cold pool gyre in the western Irish Sea, Prog. Oceanogr., 46, 1-58, https://doi.org/10.1016/S0079-6611(99)00054-3, 2000.

Kobayashi, S., Simpson, J. H., Fujiwara, T., and Horsburgh, K. J.: Tidal stirring and its impact on water column stability and property distributions in a semi-enclosed shelf sea (Seto Inland Sea, Japan), Cont. Shelf Res., 26, 1295-1306, https://doi.org/10.1016/j.csr.2006.04.006, 2006.

Lentz, S. J.: Seasonal warming of the Middle Atlantic Bight Cold Pool, J. Geophys. Res. Oceans, 122, 941–954, https://doi:10.1002/2016JC012201, 2017.

Li, A., Yu, F., Si, G., and Wei, C.: Long-term temperature variation of the Southern Yellow Sea Cold Water Mass from 1976 to 2006, Chin. J. Oceanol. Limnol., 35, 1032-1044, http://dx.doi.org/10.1007/s00343-017-6037-1, 2017.

Li, X., Wang, X., Chu, P. C., and Zhao, D.: Low-frequency variability of the Yellow Sea Cold Water Mass identified from the China Coastal waters and adjacent seas reanalysis, Adv. Meteorol., 1-14, https://doi.org/10.1155/2015/269859, 2015.

Lin, C., Ning, X., Su, J., Lin, Y., and Xu, B.: Environmental changes and the responses of the ecosystems of the Yellow Sea during 1976–2000, J. Mar. Syst., 55, 223-234, https://doi.org/10.1016/j.jmarsys.2004.08.001, 2005.

Park, K. A., Lee, E.Y., Chang, E., and Hong, S.: Spatial and temporal variability of sea surface temperature and warming trends in the Yellow Sea, J. Mar. Syst., 143, 24-38, https://doi.org/10.1016/j.jmarsys.2014.10.013, 2015.

Park, S., Chu, P. C., Lee, and J. H.: Interannual-to-interdecadal variability of the Yellow Sea Cold Water Mass in 1967–2008: characteristics and seasonal forcings, J. Mar. Syst., 87, 177-193, https://doi.org/10.1016/j.jmarsys.2011.03.012, 2011.

Simpson, S. D., Jennings, S., Johnson, M. P., Blanchard, J. L., Schön, P. J., Sims, D. W., and Genner, M. J.: Continental shelf-wide response of a fish assemblage to rapid warming of the sea, Curr. Biol., 21, 1565-1570, https://doi:10.1016/j.cub.2011.08.016, 2011.

460 Stabeno, P. J., Kachel, N. B., Moore, S. E., Napp, J. M., Sigler, M., Yamaguchi, A., and Zerbini, A. N.: Comparison of warm and cold years on the southeastern Bering Sea shelf and some implications for the ecosystem, Deep Sea Res. II, 65-70, 31-45, https://doi.org/10.1016/j.dsr2.2012.02.020, 2012.

Takeoka, H., Matsuda, O., and Yamamoto, T.: Processes causing the chlorophylla maximum in the tidal front in Iyo-nada, Japan, J. Oceanogr., 49, 57-70, https://doi.org/10.1007/BF02234009, 1993.

465 Turner, R. E., Rabalais, N. N., and Justić, D.: Trends in summer bottom-water temperatures on the northern Gulf of Mexico continental shelf from 1985 to 2015, PLoS One, 12, e0184350, https://doi.org/10.1371/journal.pone.0184350, 2017.

Wang, D., Huang, B., Liu, X., Liu, G., and Wang, H.: Seasonal variations of phytoplankton phosphorus stress in the Yellow Sea Cold Water Mass, Acta Oceanol. Sin., 33, 124-135, https://doi.org/10.1007/s13131-014-0547-x, 2014.

Wang, X., and Zhao, J.: Distribution and inter-annual variations of the cold water on the northern shelf of Bering Sea in
470 summer, Acta Oceanol. Sin., 33, 2011. (in Chinese)

Wei, H., Shi, J., Lu, Y., Peng, Y.: Interannual and long-term hydrographic changes in the Yellow Sea during 1977–1998, Deep Sea Res. II, 57, 1025-1034, https://doi.org/10.1016/j.dsr2.2010.02.004, 2010.

Yang, H. W., Cho, Y..K., Seo, G. H., You, S. H., and Seo, J. W.: Interannual variation of the southern limit in the Yellow Sea Bottom Cold Water and its causes, J. Mar. Syst., 139, 119-127, https://doi.org/10.1016/j.jmarsys.2014.05.007, 2014.

475 Yu, X., and Guo, X.: Intensification of water temperature increase inside the bottom cold water by horizontal heat transport, Cont. Shelf Res., 165, 26-36, https://doi.org/10.1016/j.csr.2018.06.006, 2018.

Yu, X., Guo, X., and Takeoka, H.: Fortnightly variation in the bottom thermal front and associated circulation in a semienclosed sea, J. Phys. Oceanogr., 46, 159-177, https://doi.org/10.1175/JPO-D-15-0071.1, 2016.

Zhang, J., Woodgate, R., and Mangiameli, S.: Towards seasonal prediction of the distribution and extent of cold bottom
480 waters on the Bering Sea shelf, Deep Sea Res. II, 65, 58-71, https://doi.org/10.1016/j.dsr2.2012.02.023, 2012.

Zhu, J., Guo, X., Shi, J., and Gao, H.: Dilution characteristics of riverine input contaminants in the Seto Inland Sea, Mar. Pollut. Bull., 141, 91-103, https://doi.org/10.1016/j.marpolbul.2019.02.029, 2019.

Zhu, J., Shi, J., Guo, X., Gao, H., and Yao, X.: Air-sea heat flux control on the Yellow Sea Cold Water Mass intensity and implications for its prediction, Cont. Shelf Res., 152, 14-26, https://doi.org/10.1016/j.csr.2017.10.006, 2018.